

# Fabrication of Analog Electronics for Serial Readout of Silicon Strip Sensors

E. Won,\* J. H. Choi, and H. Ha

*Department of Physics, Korea University, Seoul 136-713, Korea*

H. J. Hyun, H. J. Kim, and H. Park

*Department of Physics, Kyungpook National University, Daegu 702-701, Korea*

(Received January 5 2006)

## Abstract

A set of analog electronics boards for serial readout of silicon strip sensors was fabricated. A commercially available amplifier is mounted on a homemade hybrid board in order to receive analog signals from silicon strip sensors. Also, another homemade circuit board is fabricated in order to translate amplifier control signals into a suitable format and to provide bias voltage to the amplifier as well as to the silicon sensors. We discuss technical details of the fabrication process and performance of the circuit boards we developed.

PACS numbers: 83.85.Gk, 84.30.Le, 84.30.Sk

Keywords: amplifier, electronics, ASIC

---

\*Electronic address: eunilwon@korea.ac.kr; Fax: +82-2-927-3292

## I. INTRODUCTION

Over the last thirty years, there have been impressive developments in silicon strip sensors and their readout electronics in the field of elementary particle physics. They were first used more than twenty years ago for heavy flavour searches in fixed target experiments [1]. In particular, their potential use as high precision vertex detectors around high energy colliders, both for electron-positron and proton-antiproton machines, has initiated further development of high performance semiconductor detectors till now [2, 3, 4]. Subsequently, it became clear that much higher density electronics was required and it drove the construction of integrated circuit amplifiers in metal-oxide-silicon technology. Therefore, application specific integrated circuit (ASIC) technology has been heavily used in designing readout electronics for silicon sensors in the particle physics experiments [5, 6]. The interface electronics board between silicon sensors and readout ASIC chips is traditionally called hybrid boards and the experiment-specific hybrid boards have been produced for various experiments [6, 7, 8]. The design of such hybrid boards should consider cooling system for collider experiments and low electrical noise performance for detecting small signals.

Recently, research activities on the high density readout electronics have been extended to the field of high resolution medical imaging [9] as well as charged particle trackers in the future particle physics program [10]. Therefore, it becomes clear that the knowledge and experience in fabricating hybrid board and reading out analog signals from it may be one of important items for the participation to such programs. In this respect, we discuss development of several different types of hybrid boards and related electronics board with the technology available domestically. Section II describes our first prototype hybrid board. The fabrication of detector bias and dc voltage delivery for the operation of ASIC chip, and the control logic translator system is described in section III. We also fabricated a specialized hybrid board in order to test the ASIC amplifier itself and it is described in section IV. Our latest design that mounts a 17 channel single-side silicon detector is described in section V.

## II. DESIGN OF HYBRID BOARD I

In this section, we discuss the development of our first prototype of the hybrid board that mounts a commercially available high density ASIC amplifier, the VA chip [11, 12, 13]. It

has in total 128 analog channels and each channel contains a charge-sensitive preamplifier, a shaper, a track-and-hold, and multiplexing capacity. In order to communicate to the VA chip, one has to wire-bond approximately 30 lines of various analog and digital signals from the VA chip to the hybrid board. Since the width of the VA chip is 5 mm, the layout size of 30 pads on the printed circuit board (PCB) also should be in the similar size in order to make good electric connections to the VA chip. It turns out that a pad width and the pitch of pads both should be on the order of 100  $\mu\text{m}$  on the PCB in order to make a good ultrasonic wire-bonding to the VA chip. However, most of domestic, small-size vendors expressed difficulty in fabricating such fine structure PCB layout with their facility. Figure 1 shows our first attempt to fabricate high density pads on the PCB from a domestic vendor. A large rectangular hole is made on the left corner of the board where the sensor is to be mounted. This hole is placed in order to minimize the material for the future radioactive source or beam tests. The PCB is made with four layers where analog and digital grounds are routed in the same layer. One can also see a smaller, horizontally long rectangular pad (labeled as U2) near to the place for the VA chip (labeled as U1). This rectangular pad is for the  $R/C$  chip [14] as the detector to be mounted at the design stage is a dc-type sensor [15]. This complicates the detector biasing method quite significantly because the  $R/C$  chip we use is known to break down at 70 V and therefore a voltage division is made to provide full depletion bias voltage to sensors.

A tin-lead alloy was used in order to cover all copper pads on the PCB. Later we realized that in some countries there are at least directives restricting the use of lead for such purpose and therefore we abandoned the use of tin-lead alloy completely. The use of tin-lead alloy resulted in significantly bad quality in the layout of the pad outlines. A microscope picture of the pads in Fig. 2 (a) illustrates the situation. The three horizontal lines in the figure represent bonding pads on the hybrid PCB. The average width of pads (thickness in vertical direction) is always less than 15  $\mu\text{m}$  and is too narrow for any practical use. We labeled this first PCB board as the version 0.9. There is another problem in the version 0.9. The board was not flat and it prevented us from mounting silicon sensors as it does not provide mechanically stable configuration. This situation is also shown in Fig. 2 (c). After the fabrication of the version 0.9, there has been series of discussion with technicians from the vendor in order to identify source of these two problems. The problem with the poor quality of the pad outline is partially solved by modifying one of chemical etching processes

in their PCB fabrication. We also use gold to cover all copper pads on the PCB and it partially helped in improving the quality of the bonding pad. The source of the non-flat structure of the board was due to improper handling of the PCB during the cooling process. After identifying sources of troubles mentioned above, we fabricated our second prototype hybrid board with minor modification as far as the design is concerned. A placeholder for a lemo connection to the analog signal output is made for debugging purpose in the second prototype. Figure 2 (b) shows the quality of the pitch for the second prototype board. Measurements showed that the width of pads is  $110\ \mu\text{m}$  which satisfies our specification. The trouble with the non-flatness of the board is also disappeared in the second prototype and it is clearly shown in Fig. 2 (d). We label the second prototype as the hybrid version 1.0. We note that in order this to be used in the real collider environment, it has to deal with the heat generated during the collision. One of solutions is to make the PCB with ceramic material but we did not investigate the possibility of making ceramic PCB at this time for a quick development of the board.

There are in total twenty passive surface-mounted components soldered on the hybrid board. All components are a  $F$ -class which has  $\pm 1\%$  tolerance from their specification values. A conductive epoxy from Chemtronics CW2400 [16] is tested for a good ohmic contact with the gold pad on the hybrid board and is used in order to mount the VA chip on the hybrid board, as the bottom plate of the VA chip requires an electric contact. After through electrical tests, assembled hybrid boards are shipped to a local company [17] for an ultrasonic wire-bonding between the VA chip and the hybrid board. After the wire-bonding, the hybrid boards are delivered back to the laboratory and a readout setup is made to communicate with the hybrid board. A dc power supply is connected to a homemade electronics board in order to provide voltage and current sources to the hybrid board. We discuss the detailed design of this second homemade board in the following section. The control signals are generated from a commercially available field programmable gate array (FPGA) test board from Xilinx [18]. It has a SPARTAN XC3S200 on the board and a very high speed integrated circuit hardware description language (VHDL) firmware is written by us in order to generate LVCMOS control logic signals to be sent to the VA chip. The detailed time structure of these control signals may be found from the reference [12]. The indication of a successful communication with the VA chip may be the presence of a return signal from the VA chip. To be more specific, when all 128 channels are serially read out,

there is a signal coming from the VA chip, indicating a serial data readout is completed. In the reference [12], it is referred as `shift_out` and we confirmed that we were able to see this line became active-low, immediately after all 128 channels were read out. Figure 3 (a) and (b) show the behavior of the analog output and the `shift_out` signals, captured in an oscilloscope from a commercially available VA evaluation board [13] that was tested by us, and from our homemade hybrid board version 1.0. The well-like signals in Fig. 3 (a) and (b) show the analog outputs from the evaluation board and our hybrid board version 1.0, respectively. Since the evaluation board we purchased has two VA chips on the board, the width of the well from the evaluation board in Fig. 3 (a) is twice larger than the width from the hybrid board version 1.0 in Fig. 3 (b). At this stage, both boards have no sensors mounted and therefore the analog outputs are pedestals only. The other signals in Fig. 3 (a) and (b) are `shift_out` and should be active-low at the end of the serial readout of the VA chip. Such behavior can be clearly seen from the zoomed view in Fig. 3 (c) for the evaluation board and (d) for the hybrid board version 1.0, respectively. It appears that cross-talk from the clock signal at the edge to the analog output signal is somewhat worse in the hybrid board 1.0, as indicated in Fig. 3 (c) and (d). We attribute that it is originated from the ground routing issues in the PCB design or imperfect impedance matching but no conclusive statement can be made at this moment without further study.

### III. DESIGN OF POWER, LOGIC TRANSLATORS AND CURRENT SOURCES

In order to operate the VA chip, one has to provide several voltage and current sources, and non-standard control logic signals for serial readout and calibration purposes. Also, bias voltage for the silicon sensors has to be provided as well. In order to provide power, logic translators, and current sources (PLC), we developed another homemade electronics called PLC board. We started with a hand-soldered prototype which is shown in Fig. 4. There are four dc power lines connected to the PLC board:  $\pm 6.6$  V for the main power that operates components mounted, +4 V for the sensor bias voltage, and +16 V for the extra bias for p-stop in the sensor we were planning to mount at the design stage. In order to bias the silicon sensors, a dc to dc converter is designed using the EMCO high voltage chip Q01-05 [19]. This model was chosen in order to provide positive and negative voltages simultaneously due to the fact that the *R/C* chip was used in the hybrid side. The VA chip

control signals are originally generated from the outside of the PLC board and are fed into the PLC board as LVCMOS logic. The PLC receives the control signals and translate them into a new logic with logical one begin  $+1.5$  V and zero  $-2.0$  V. Once it is done, signals are transferred to the hybrid board. Another functionality in the PLC board is that the differential analog output from the VA chip is changed to a single-ended signal through an analog receiver. This may be the source of the noise that appears in following sections.

After careful studies on this prototype, a PCB is fabricated and a picture of it is shown in Fig. 5. It has 6 layers and most of the components are chosen to be surface mountable type, in order to reduce the size of the board. The physical dimension is  $84 \times 84$  mm. The analog and digital powers are now separated in the PCB version of the PLC board and it enables us to reduce the noise due to the digital clock. There are two square layouts on the PCB which are left blank in Fig. 5. Two EMCO high voltage chips are mounted on the back side of the board due to the mistakes in the design of the PCB.

With this PLC board, the VA chip is tested in a calibration mode. An external coupling capacitor is connected to the calibration input and test pulses are generated in order to store electric charge to the capacitor. The channel to be tested is selected prior to the charge injection and the amplified signal comes out without serialization of the data. In this sense, the calibration is somewhat different from the serial signal readout from the sensor. Figure 6 shows the response of the VA chip for different test pulse values in mV. In this test, one MIP corresponds to 3 mV. A good linearity is achieved up to 7 MIPs, indicating a good performance of the VA chip with our assembled electronics. According to the VA chip specification, the dynamic range reaches to  $\pm 10$  MIPs but the goal of our study is to develop the electronic boards and therefore we did not test the full dynamic range of the VA chip in this study.

#### IV. DESIGN OF HYBRID BOARD II

Due to the fact that the delivery of sensors are behind the schedule, we decided to design another hybrid board that allows us to test the readability of the VA chip without real sensors. We label this one as VA-test hybrid board. In this board, the rectangular hole for the sensor mounting is removed, as indicated in Fig. 7. Instead, we place a set of wire-bond pads on the board near to the input sides of the VA chips to be mounted. One may see such

configuration in Fig. 7, left side from the layouts for the VA chips. And then, direct wire-bonding from these pads to the input pads on the VA chip is made in order to inject electric charges to the VA chip. This is practically same method as the charge injection using the real sensor attached to the VA chip. This method is however somewhat different from the calibration mode mentioned in the previous section because in the calibration process, there is no holding of the charge inside of the VA chip and no serialization of the data is carried out. A lemo connector is prepared in order to inject electric charges using an external pulse generator and channel selection is made through hand-soldering to the pads to be tested, one at the time. Using this technique, one MIP “signal” is generated and the measured voltage output is shown in Fig. 8. The bump on the left corresponds to the pedestal of the entire electronics and the other bump on the right is one MIP signal. The measurement was done directly from the oscilloscope by measuring the voltage outputs from the hybrid board. From the fits to two bumps, the signal-to-noise ratio was measured to be 14. This is worse than the nominal values one may get with the silicon sensors. One of the reasons may be due to the fact that the electronics noise is larger. We discuss it in detail in the next section. The equivalent noise charge (ENC) is measured to be  $1740 e^-$  ENC with an 1 pF coupling capacitor and again this is a significantly worse value than the value in the specification,  $180 + 7.5/\text{pF} e^-$  ENC [13]. We discuss a possible reason for this in the next section.

In this VA-test board, we also tested serial readout of multiple VA chips. For this test, two VA chips are daisy-chained and in total 256 channels are read out. We confirmed that the analog output behaves similar to described in Fig. 3 (a) where two VA chips were mounted on the evaluation board that we tested. We also injected a test pulse to the second VA chip and successfully read out signals from it.

## V. DESIGN OF HYBRID BOARD III AND BEAM TEST

Based on the experience gained from studies described in previous sections, we designed our hybrid board version 2.0, shown in Fig. 9. This time, a 17 channel single-sided silicon detector (SSD) [15] is mounted. Also, in order to avoid the complexity in biasing the detector due to the  $R/C$  chip, we decide to make an array of surface-mount resistors and capacitors to compensate leakage current. The version 2.0 has in total 6 layers in the PCB including a

power and a ground plane. One VA chip is hand-mounted with the conductive epoxy in the laboratory and all necessary wire-bonding processes are done from the company [17]. Note that there are only 17 channels that are wire-bonded from the sensor to the VA chip. All electrical tests are carried out and show no trouble.

In order to measure real signal from the charged particle, a beam test is carried out at Korea Institute of Radiological and Medical Science (KIRAMS). A small proton cyclotron with an energy of 35 MeV is used for the test with the beam current ranging from 0.3 nA to 10 nA. Here, we discuss the performance of the electronics only and detailed performance of the sensor will be addressed in a separate paper. First, the width of the pedestal we measured at the laboratory is similar to the level at KIRAMS when the proton beam is present, indicating the electronics does not become noisy in environment such as the beam area. Then the detector is fully biased and the signal is read out using the data acquisition system we prepared. A trigger signal comes from a 30 ml liquid scintillator that is made of 10 % of BC501A and 90 % of mineral oil loading [21]. A 12 bit 40 MHz Versamodule Eurocard (VME) flash analog-to-digital converter (FADC) is used to digitize the analog output signal from the hybrid board. A VME CPU running a linux operating system collects data stored in a 4K word long buffer inside of the FADC. The ROOT [20] package is interfaced with a VME device driver that controls VME slave boards and the data are stored in a ROOT format for offline analysis. A clocked raw output from the hybrid board is shown in Fig. 10 (a). It has two sharp peaks and their positions correspond to the channels that were wire-bonded to the VA chip. These two peaks may correspond to the proton beams detected by the silicon strip sensor. However, we observe undershooting of the clocked analog outputs. The zoomed view of the peak is in Fig. 10 (b) with the clock signal shown in Fig. 10 (c). A clear undershooting exists over a clock period. It appears that the source of the undershooting may be from the driver chip on the PLC board that converts differential analog output from the VA chip to single-ended signal. It turns out that the speed of the driver chip was much slower than the clock speed of the VA chip operation which was 4 MHz for the beam test. This may explain a larger noise observed in the signal-to-ratio measurement shown in the previous section.

## VI. CONCLUSIONS

A series of electronics boards are fabricated in order to serially read out small analog signals from high density sensors such as silicon strip detectors. A commercially available amplifier is mounted on a homemade hybrid board in order to receive analog signals from the detectors. Fabrication of the board, micro-patterning of pads for ultrasonic wire-bonding, and necessary wire-bonding on the hybrid board are carried out and tests show a good performance of the fabricated board. Also, a compact electronics board that provides necessary current, voltage source, and control logic is fabricated in order to communicate with the hybrid board. The linearity of the VA chip is studied in the calibration mode and a good response is achieved up to 7 MIPs. A VA-test hybrid board is fabricated and the signal-to-noise ratio is measured with somewhat worse ENC value than the specification value. We expose the electronics and silicon sensors in the proton beams and verified a good performance of the electronics in the beam environment. However, the noise value is higher than the nominal value and there is undershooting in the analog output signal. It turns out that the speed of the driver chip on the PLC board may be too slow for our application. These problems will be examined in future and will be addressed in a separate paper. The electronics boards discussed in the paper may be used in applications including medical imaging and charged particle tracking system with no thermal dissipation is required. Fabrication of the hybrid board with a ceramic PCB will be studied in future.

### Acknowledgments

This work is supported by grant No. R01-2005-000-10089-0 from the Basic Research Program of the Korea Science & Engineering Foundation and supported by the Korea Research Foundation Grant funded by the Korean Government (MOEHRD) (KRF-2006-C00258 and KRF-2005-070-C00032). EW is partially supported by a special startup grant from SK Corporation and by a Korea University Grant.

---

[1] Proc. 3rd, 4th and 5th Europ. Symp. on Semiconductor Detectors, Munich, Nucl. Instr. and Meth. A **226** (1984); A **253** (1987); A **288** (1990).

- [2] F. Bedeschi, F. Bedeschi, S. Belforte, G. Bellettini, L. Bosisio, F. Cervelli, G. Chiarelli, R. DelFabbro, M. Dellorso, A. DiVirgilio, and E. Focardi, *IEEE Trans. Nucl. Sci.* NS-33 (1986).
- [3] M. Hazumi, *Nucl. Instr. and Meth. A* **379**, 390 (1996).
- [4] A. Sill, *Nucl. Instr. and Meth. A* **447**, 1 (2000).
- [5] G. Hall, *Nucl. Instr. and Meth. A* **541**, 248 (2005).
- [6] M. Feuerstack-Raible, *Nucl. Instr. and Meth. A* **447**, 35 (2000).
- [7] M. Tanaka, M. Hazumi, J. Ryuko, K. Sumisawa, and D. Marlow, *Nucl. Instr. and Meth. A* **432**, 422 (1999).
- [8] A. Rahimi, K. E. Arms, K. K. Gan, M. Johnson, H. Kagan, C. Rush, S. Smith, R. Ter-Antonian, M. M. Zoeller, A. Ciliox, M. Holder, S. Nderitu, and M. Ziolkowski, *International Journal of Modern Physics A*, **20**, 3805 (2005).
- [9] G. J. Royle, A. Papanestis, R. D. Speller, G. Hall, G. Iles, M. Raymond, E. Corrin, P. F. van der Stelt, N. Manthos, and F. A. Triantis, *Nucl. Instr. and Meth. A* **493**, 176 (2002).
- [10] E. Won, H. Ha, S. K. Park, and Y. I. Kim, *J. Korean Phys. Soc.* **49**, 52 (2006).
- [11] E. Nygard, *Nucl. Instr. and Meth. A* **301**, 506 (1991).
- [12] O. Toker, *Nucl. Instr. and Meth. A* **340**, 572 (1994).
- [13] IDEAS, Snaroya, Norway.
- [14] J. Fast for the CLEO collaborations, *Nucl. Instr. and Meth. A* **435**, 9 (1999).
- [15] J. Lee, Dong Ha Kah, Hong joo Kim, Hwan Bae Park, and Jung Ho So, *J. Korean Phys. Soc.* **48**, 850 (2006).
- [16] Chemtronics, Kennesaw, GA, USA.
- [17] LP electronics, Seoul, Korea.
- [18] Xilinx Corporation, San Jose, CA, USA.
- [19] EMCO High Voltage Corporation, Sutter Creek, CA, USA.
- [20] R. Brun and F. Rademakers, *Nucl. Instr. and Meth. A* **389**, 81 (1997).
- [21] Private communication with H. J. Kim.

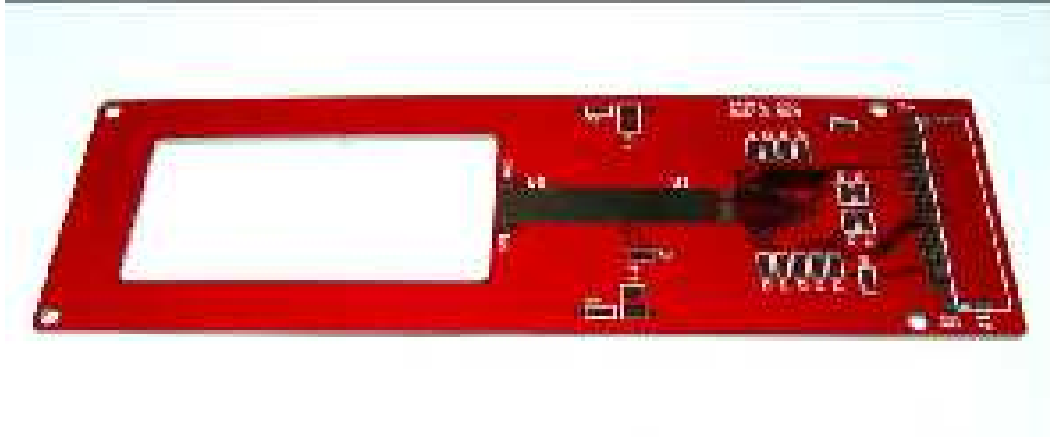


FIG. 1: A picture of the hybrid board version 0.9. A large rectangular hole on left is prepared for future beam or radioactive source tests when a sensor is mounted on the hybrid board. U1 is the pad for the VA chip and U2 is for the  $R/C$  chip.

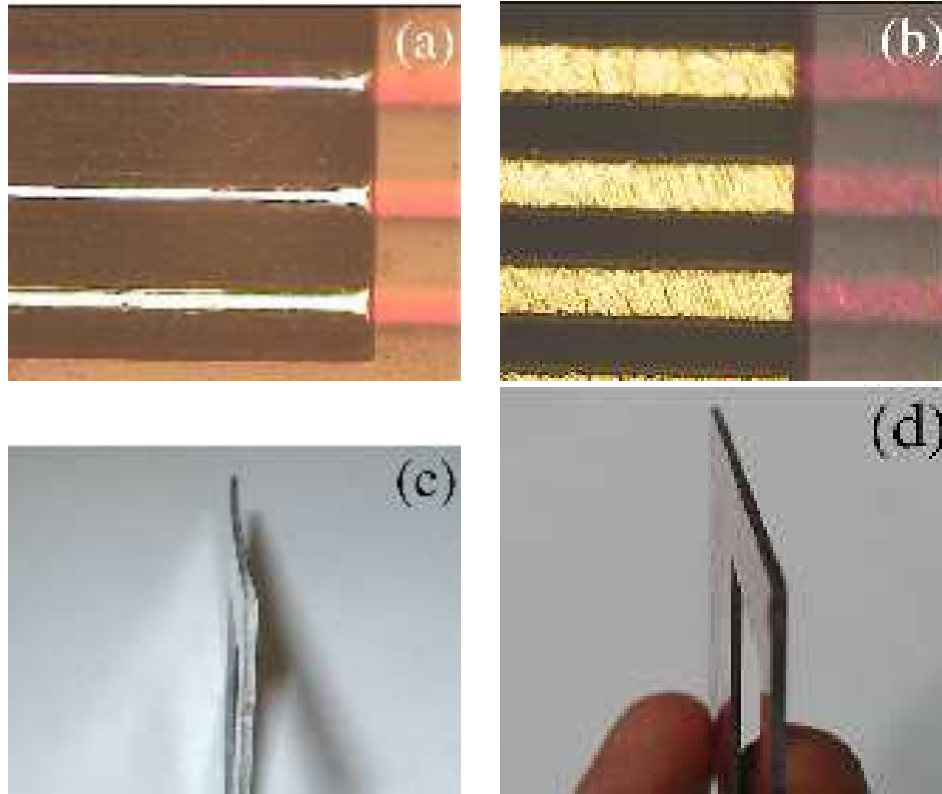


FIG. 2: Zoomed views of hybrid board version 0.9 and version 1.0. Microscope picture of the bonding pad on the board is shown in (a) for the version 0.9 and in (b) for the version 1.0. They are in same scale and clear improvement in the quality of the layout can be seen in (b). Side views of the boards are shown in (c) for the version 0.9 and in (d) for the version 1.0.

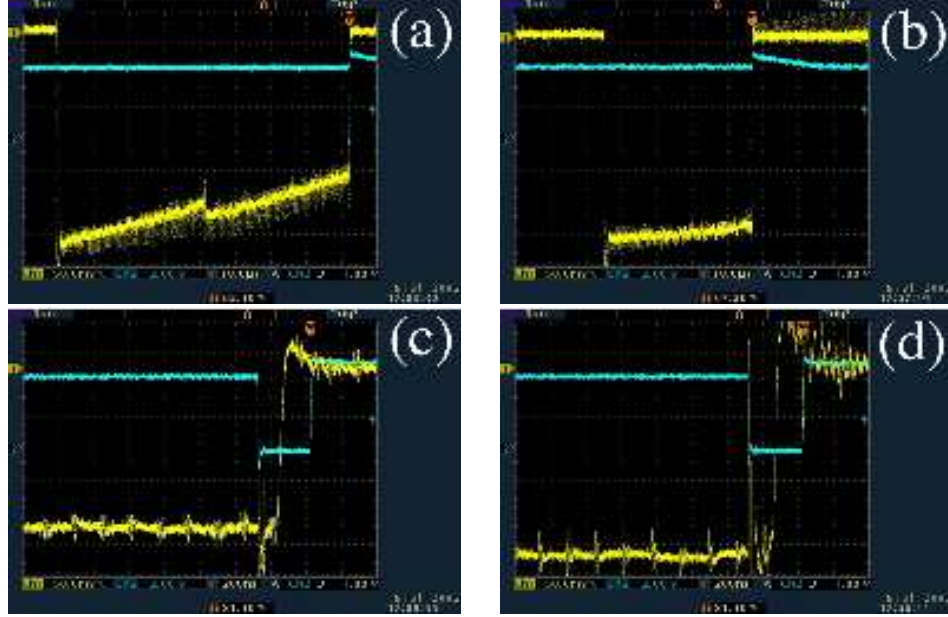


FIG. 3: Analog and digital output signals from the VA chip captured in the oscilloscope. A distorted well-shape signal in (a) and (b) are the analog outputs from the evaluation board provided by the company and from our hybrid board version 1.0, respectively. The evaluation board houses two VA chips and the width of the well in (a) reflects it. The other line in each figure is the digital control signal (`shift_out`) indicating the end of the serial readout. (c) and (d) are zoomed views of (a) and (b) at the rising edge of the analog out.

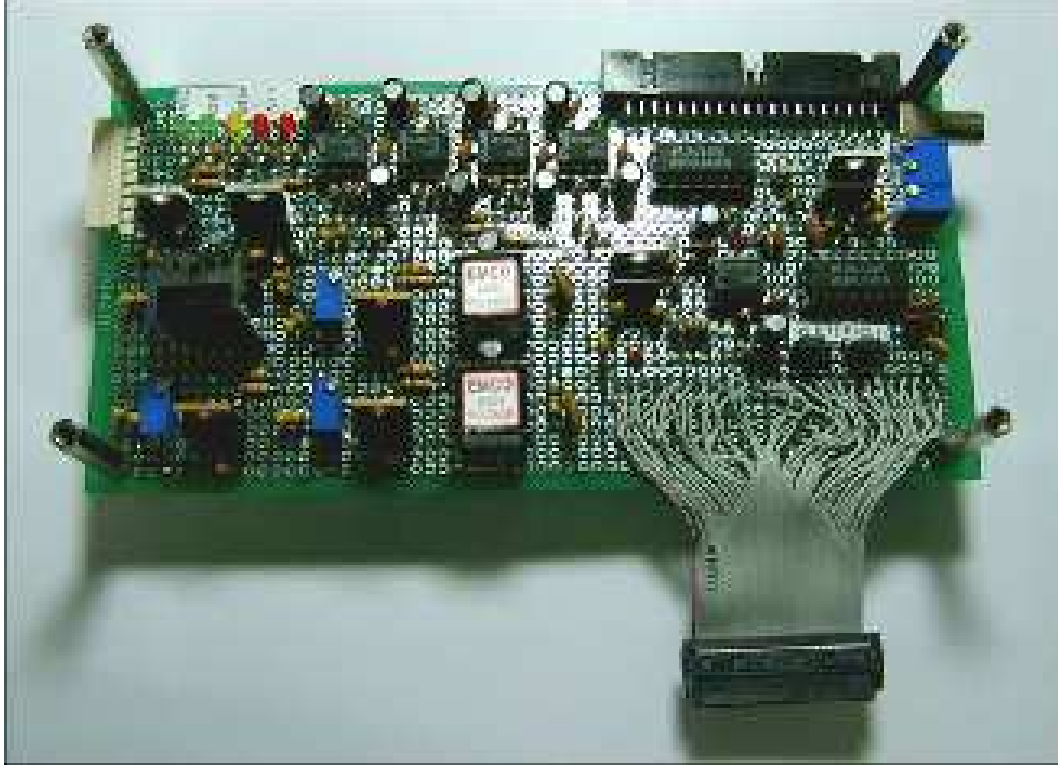


FIG. 4: A picture of the PLC board prototype with hand-wirings. A micro-connector at the bottom right is for the hybrid board, the one on the top-right is for the commercial evaluation board with a FPGA, and the one on the top left is for dc power connection.

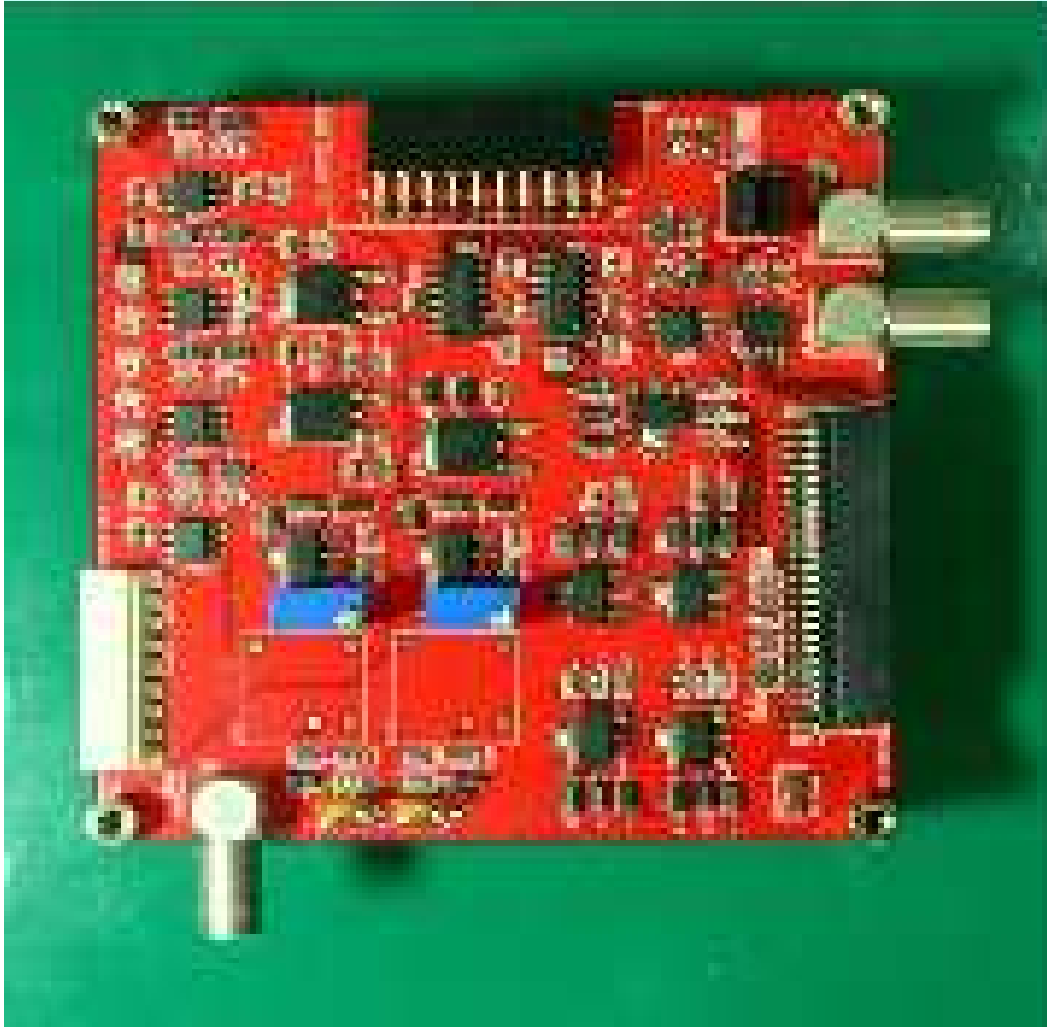


FIG. 5: A picture of the PLC board fabricated with a standard PCB process. The physical size is  $84 \times 84$  mm. A micro-connector at the bottom right is for the hybrid board, the one on the top is for the commercial evaluation board with a FPGA, and the one on the left is for dc power connection. All the components are chosen to be surface mountable in order to reduce the size of the board.

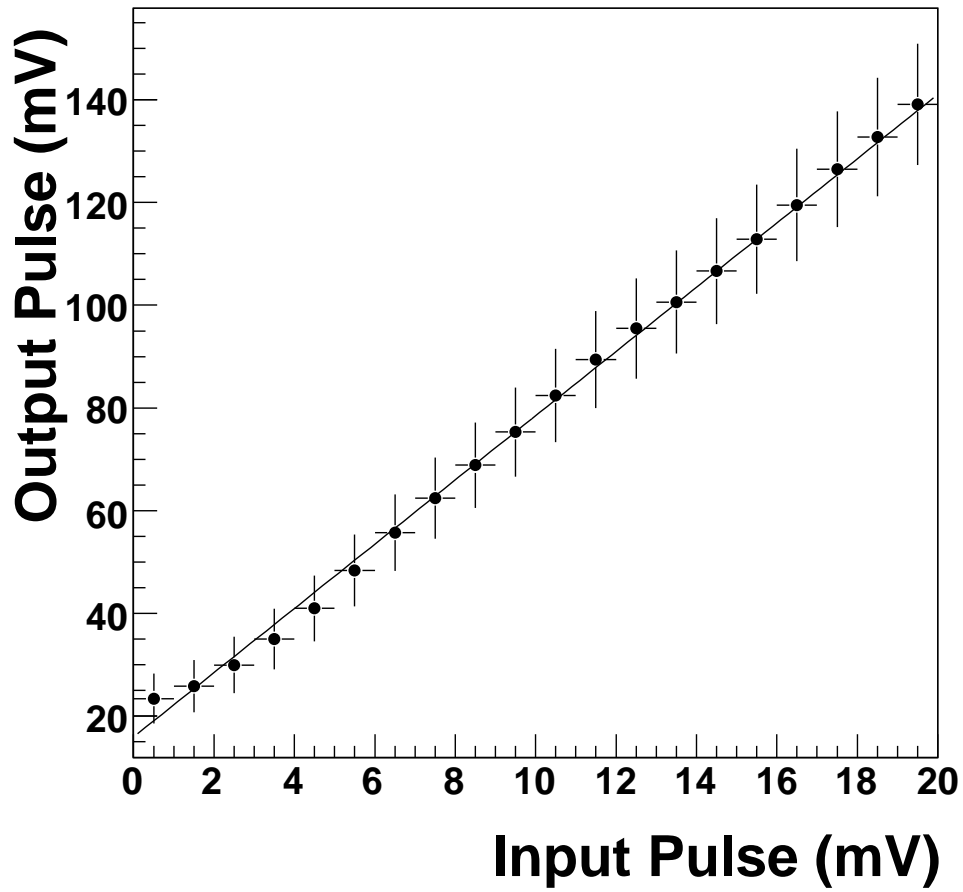


FIG. 6: A response of the VA chip and hybrid board version 1.0 on test pulses when the VA chip is in the calibration mode. Here, an input test pulse of 3 mV corresponds to 1 MIP signal.

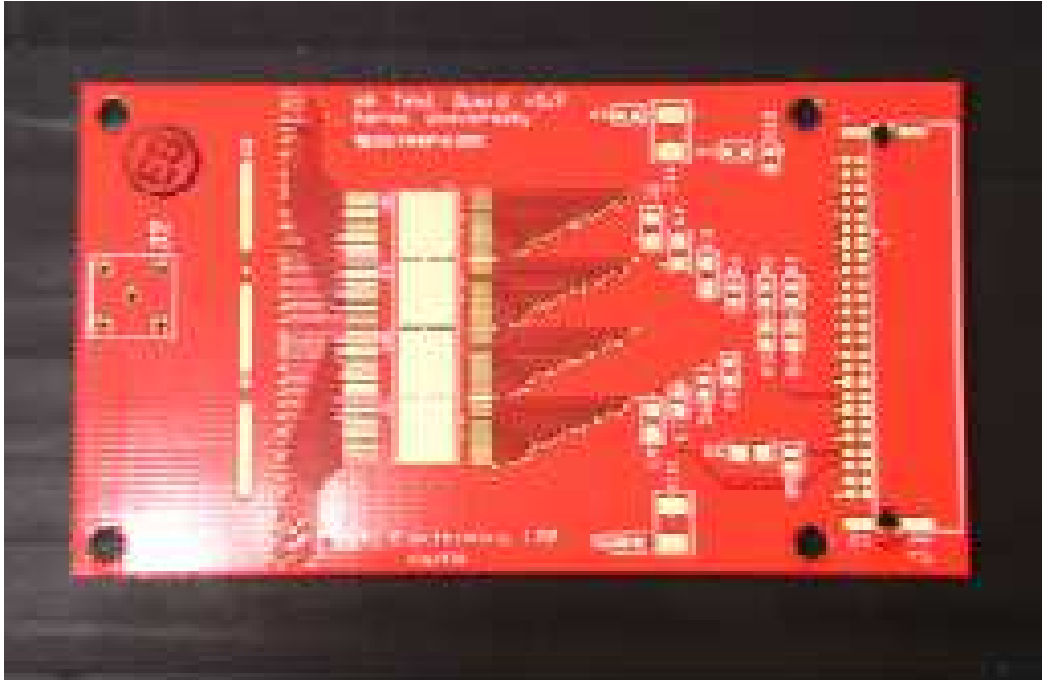


FIG. 7: A picture of the VA-test board. This board is designed to mount in total four VA chips. Selected channels in the VA side can be wire-bonded to pads on the PCB for a direct delivery of current signals from an external pulse generator.

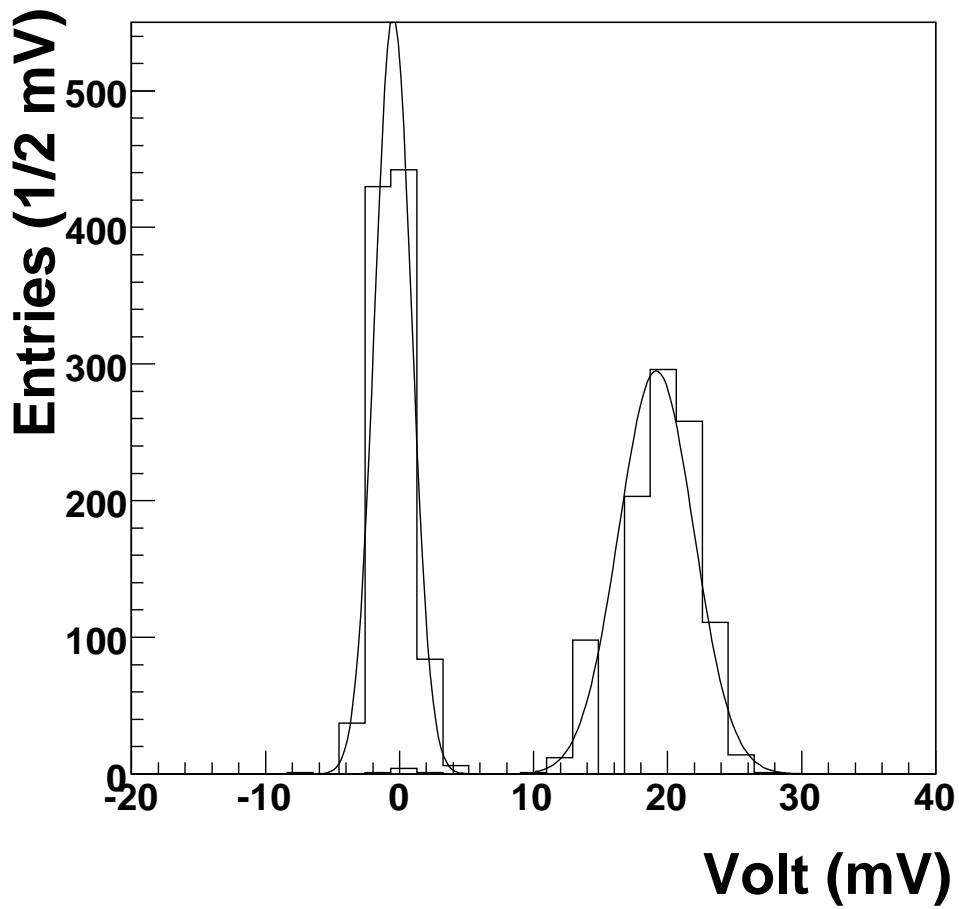


FIG. 8: Distribution of the measured analog output from the VA-test board when a test pulse of one MIP signal is injected. The signal distribution is on the right and the pedestal peak is shown on the left. The measurement was done directly from the oscilloscope by measuring the voltage outputs from the hybrid board.

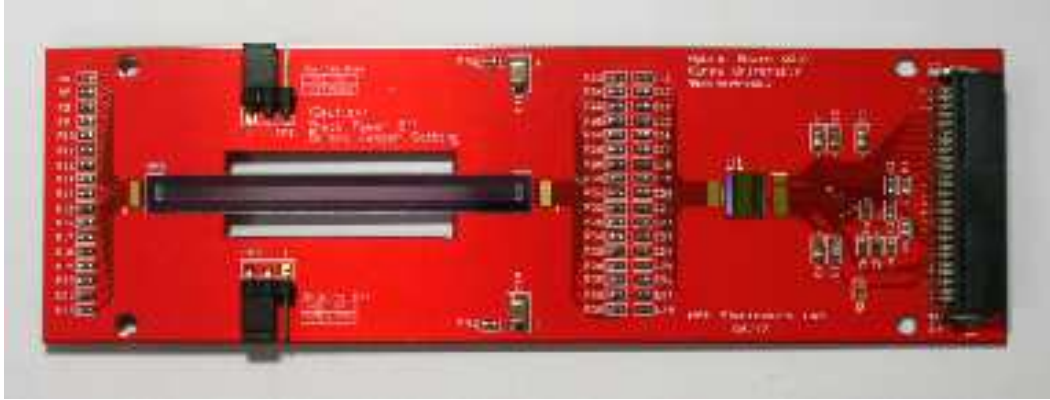


FIG. 9: A picture of the hybrid board version 2.0. A 17 channel single-sided silicon sensor is mounted on the left side. Surface-mounted resistor and capacitor arrays are placed in order to compensate dc current in order to replace the  $R/C$  chip.

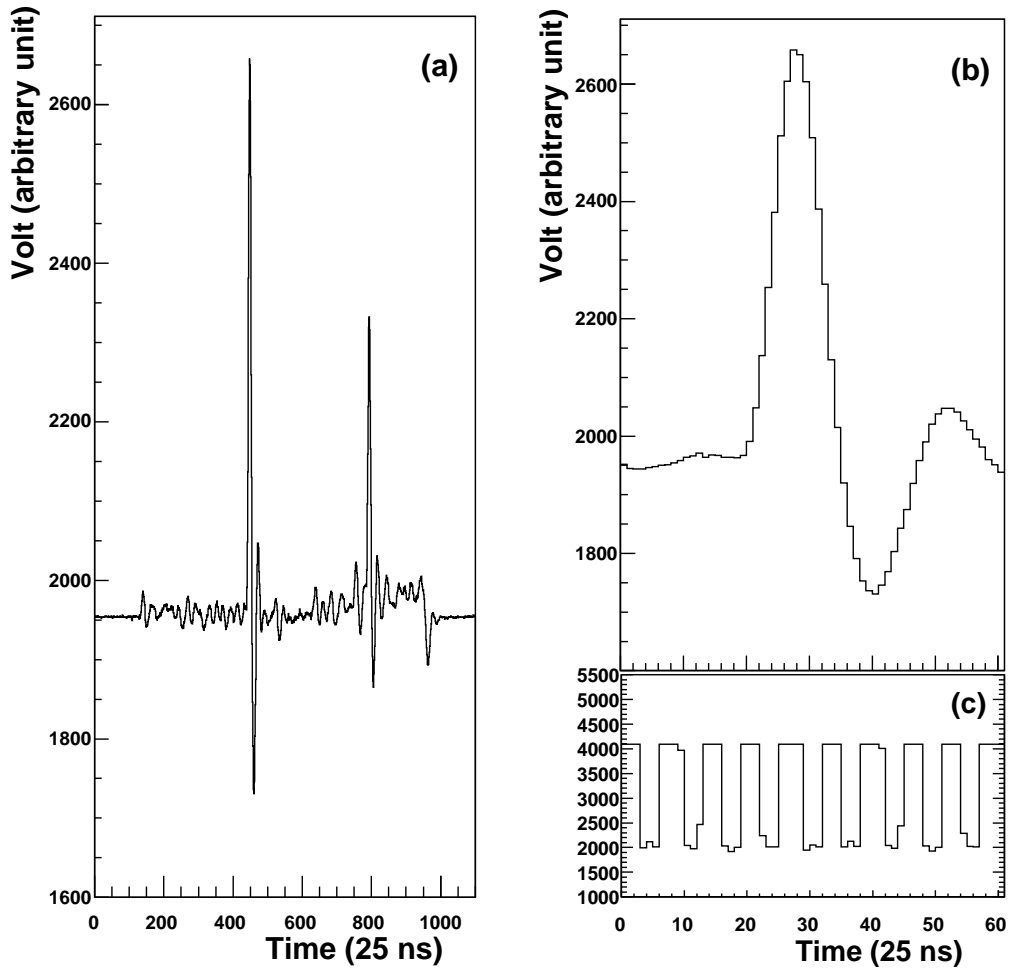


FIG. 10: Analog output and clock signals from the hybrid board. The analog output from the VA chip over 128 channels is shown in (a) where the readout clock starts at 100 and ends at 950 counts in the horizontal axis. A zoomed view of the first peak in (a) is shown in (b) where an undershooting is clearly visible. The time synchronized clock signal fed into the VA chip is also shown in (c).